Developing an Automated Algorithm Detection of Micro Aneurysms in Images of Retina for The Purpose of Early Diagnosis of Diabetic Retinopathy

Student Name:

AHMED SALEM ALRASHDI

Supervised By:

Prof Murk Bottema

Submission Date:

25/7/2016

Submitted to the School of Computer Science, Engineering, and Mathematics in the Faculty of Science and Engineering in partial fulfilment of the requirements for the degree of Master of Biomedical Engineering at Flinders University - Adelaide Australia

The Declaration

I certify that this work does not incorporate without acknowledgment any material previously submitted for a degree or diploma in any university; and that to the best of my knowledge and belief it does not contain any material previously published or written by another person except where due reference is made in the text.

Signature

Acknowledgment

I would like to express my special thanks to my supervisor Prof Murk Bottema for his support and encouragement during my thesis period. His guidance and supervision helped me to complete this project. I learned many researching skill and develop my understanding in the project area.

Secondly, I would like to appreciate the help and support from my family to finalize this project on the limited time frame.

ABSTRACT

Diabetes is one of the leading problems not only faced by persons aged 25-74 years but it is spreading in young generations too. Diabetes can cause inability of the eye to focus with the increase of diabetes from moderate to severe conditions. This symptom leads to optometrist's diagnosis of patients. Several years of increase of Diabetes in a person leads damage of vision and can even cause blindness. These various factors lead towards the study of Diabetic Retinopathy. The extract mechanism which leads to Diabetic Retinopathy is given in various studies, but still there is a need to study and formulate the typical problem and its history.

The motivation for this work includes the provision of detection of retinopathy in its early stage so that the prevention steps could be taken and hence protects the vision of a person suffering from diabetes. Microaneurysms (MAs) are defined as the first stage of retinopathy in which we find the red spots in the superficial layer of retina walls. A model has been proposed as a new, alternative method construct profiles of the image intensity centred on the candidate MA in various directions. The main challenge in detection of MA is to find the difference between the true positives and false positives in such a way that accurate detection is available at the output.

In the past few years a large number of algorithms for candidate MA detection have been developed. A broad range of detecting algorithm follows morphological and non-morphological schemes. However, many of the methods, proposed previously failed to give good performance at the output. Istvan Lazar and Andras Hajdu [2013] proposed a method where candidate MA have been identified. In the paper, the authors then construct profiles of the image intensity centered on the candidate MA in various directions.

A new scheme to make some improvement on this is to model the intensity at candidate MA as the function. In the proposed scheme, for a single direction θ, we use logarithmic regression to fit the data on a line in direction θ to the model to obtain a number $\lambda(\theta)$. This is repeated for several directions $\theta 1, \theta 2, \ldots, \theta n$. If the candidate MA is really an MA, then all the $\lambda(\theta i)$ should be fairly large and about the same size. If the candidate MA is really due to the crossing of two vessel crossings, then the $\lambda(\theta i)$ will vary greatly. By taking the Fourier transform of the function λ, the pattern of oscillation becomes rotation invariant. Thus local maxima

are classified as a true MA or not based on the Fourier transform of lambda. One advantage of the Fourier transform is that it shifts invariant and in this case θ invariant. Thus the orientation of any background structure such as vessels is removed. For a true MA, nearly all the energy should appear in the DC component of λ. For a candidate MA that is due to the crossing of two vessels, substantial energy should appear in other Fourier coefficients. Testing which of these two methods works better and finding out how many Fourier coefficients to use is be part of the study.

TABLE OF CONTENTS

CHAPTER 3

PERFORMANCE EVALUATION

CHAPTER 4

RESULTS & DISCUSSIONS

CHAPTER 5

SUMMARY AND FUTURE STUDY

LIST OF FIGURES

LIST OF TABLES

LIST OF ABBREVATIONS

DR	Diabetic Retinopathy
MA	Microaneurysm
MAs	Microaneurysms
DME	Diabetic Macular Edema
PDR	Proliferative diabetic retinopathy
H	Haemorrhage
NPDR	Non- Proliferative diabetic retinopathy
OCT	Optical coherence tomography
MSCF	multi-scale correlation filtering
GUI	Graphical User Interface
ROC	Receiver Operating Characteristic
k-NN	*k*-Nearest Neighbours algorithm
CAD	Computer-aided diagnosis
DIARETDB1	Standard Diabetic Retinopathy Database Calibration level 1
2D	Two-Dimensional
FROC	free-response receiver operating characteristic
FFT	Fast Fourier Transform
RGB	Red-Green-Blue

CHAPTER I: INTRODUCTION

1.1 Overview

Admitting the fact of having miracle advances in the world of medicine and awareness in pathophysiology of diabetes mellitus last 25 years have been devoted to the study of Diabetic Retinopathy (DR) and many strategies came in limelight to avoid it in the person's body. Research shows that in present time DR remains one of the main cause leading to visual loss [1]. Widespread presence of DR is found in working age people who are ordeal with diabetes from a long period of time. DR is defined as a diabetic eye disease which harm the retina due to diabetes, hence leads to blindness. DR is categorized as a systemic disease (A disease which upset the normal working body organs and tissues or affects the whole physique) which become severe problem with extensive growing of diabetes for more than 20 years [1]. In the United States, according to a research report, it has shown that DR plays the major role in optic seeing which ultimately leads to blindness among the working age population approximately from 20 to 64 years. DR can be considered as a widespread and severe disease that occurs as the manifestation of either diabetes type 1 or diabetes type 2 on the retina. The disease occurs as a result in higher levels of blood glucose levels that ultimately damage the capillaries [2].

1.2 Instigation and Risk Factors of Diabetic Retinopathy

Inveterate high blood sugar because of diabetes and the long stay of it in one's body gradually may harm the tiny blood vessels of retina leading to a disease called Diabetic Retinopathy. DR can cause capillaries in the retina to leak fluid or haemorrhage spurt and injure the range of view [3]. with the period of time, new unexpected blood vessels multiply on the regions of artery walls giving path to scarring and cell loss in the retina. Usually DR is divided into stages:

1. **Mild non-proliferative retinopathy:** Small portions in the retina will convert into small balloon-shaped puffy areas disturbing the normal functioning of tiny blood vessels, is the starting foundation of DR known as MAs [3], this is the earliest stage of the disease called as mild non-proliferative retinopathy. The appearance of this stage result in a fluid leaked into the retina.

2. **Moderate non proliferative retinopathy:** In the second stage, disease is progressed when healthy blood vessel nurtured by retina may swell and distort. Deficiency of carriage cause blood rises. These circumstances leads to the inherent changes and misshape the retina welcoming the diabetic macular Edema (DME). Augmentation of fluid in the region of retina known as macula because of leaking blood vessels is known as DME. Macula is an oval yellowish area of the eye area whose work is to control the strength of vision [3]. DME becomes the reason for vision loss in people prolong to diabetes and diagnosed as moderate stage of diabetic retinopathy. Double vision, unclear or inflated vision are the signs of second stage DR which follows to blindness if not treated well on time.
3. **Severe non-proliferative retinopathy:** In third stage, the leakage in artery walls reduces the blood supply to regions near the retina due to the multiplication in the blockage of blood vessels which creates obstacles in proper vision [3]. This is the severe stage of retinopathy and needs immediate attention.
4. **Proliferative DR(PDR):**This is the very ripe stage of retinopathy where the retina triggers lead to the propagation of new delicate blood vessels widespread in the interior of the retina like a transparent gel, which fills in the eye [3]. These advancements in blood vessels are sensitive and delicate cause the leakage in the retina region. Along with the defected tissue is the reason for contraction in muscles and causes retinal detachment—as dragging away the retina from its original position in the eye. It could be compare as peeling the sticker from a sticker book. Retinal pulling out from underlying tissue can lead to permanent blindness. Figure 1.1 and 1.2 shows the difference between a normal retina and DR corrupted retina.

Figure1.1: A normal Retina

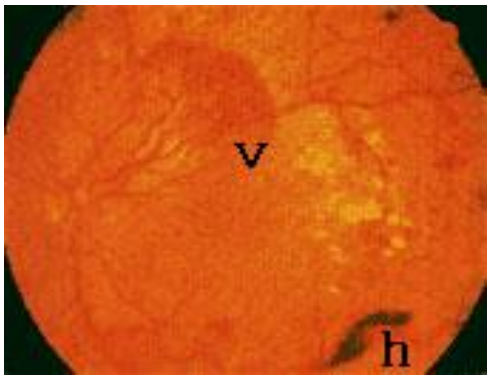

Figure 1.2: retina showing proliferative retinopathy at (v) and (h) points

Risk of the fourth stage of DR can be possible in any stage of diabetes (type 1, type 2, and gestational). As the period of diabetes increases in the person the risk of being in contact in this systematic disease increases. In a survey report conducted in America shows a surprising result that between 40 –to- 45 percent of residents are having diabetic problem with little, mild or severe stage of DR and only about half of the people are aware of it [4]. The risk is greater in pregnant women having diabetes and abrupt appearance of diabetic retinopathy. It affects to both the unborn baby and mother's health.[5].

Criteria used for grading DR can be categorized as by the following table:

DR Stage	Grades	Microaneurysm (**MA**)	Haemorrhage (H)
No DR	0	0	0
Mild	1	1<= MA <= 5	0
Moderate	2	5 – 15	0-5
Severe	3	≥ 15	>5

Table 1: summary of the type of DR stages where the values in the table are counts of the items indicated at the top of the columns

1.3 Symptoms and Detection

In the early stage of diabetic retinopathy, a person may have no symptoms, but as the person progress with diabetes, bleeding from abnormal retinal blood vessels sometimes makes objects appear as floating or blurred (Figure 1.1 and 1.2).

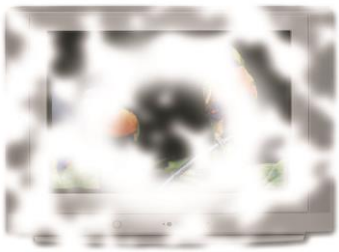

Figure: 1.3(a) ***Figure: 1.3(b)***

Figure 1.3(a) and 1.3(b) images give an impression of what someone with DRmay see compared to someone with normal vision.

Figure 1.1(a) and figure 1.2(b) shows the difference between the two images. If the treatment is ignored in this stage it leads to permanent impaired of vision.

1.3.1 Clinical Diagnosis of Diabetic Retinopathy

Diagnosis in the early stage can help in recovery from DR. DR and DME are detected with proper eye examination from the experts and with proper equipment's. Following steps shows advanced eye examination for detecting the stage of DR. Visual acuity testing is a chart used to measure the extent of person's eye vision at different distances.

1. **Tonometry.** For investigating the pressure inside the regions of eye tonometry test is performed [4].
2. **Pupil dilation.** To further examine the eye ophthalmologist puts some drops in the eye surface which broaden the area of the pupil. This is necessary for deep look inside the eye, checking retina and optic nerve and formulate the problem [4].
3. **Optical coherence tomography (OCT).** in this procedure, detailed examination of the eye is made by using the light waves so as to view and take images of tissues inside the body. OCT is a good idea to have a deep look inside the regions of eye by penetrating the light waves [4].

If DME or severe DR is indicated, a medical procedure, known as fluorescein angiography, is taken in which a fluorescent dye is used for scanning by infusing it in the body to check if the person is having some stage of DR [6]. In the early stage of DR, the patient does not realize of any vision problems but the problem increases with the degree of severity of stage. Hence the patient with diabetes is always recommended for the regular eye-check by ophthalmologist to have a check on it. NPDR can be detected

by a medical procedure known as fundus photography, in which first stage as explained above can be seen.

1.4 Significance of the Study

Early stages of diagnosis and proper treatment of the disease can help in preventing 98 percent of blindness and visual loss [7]. Periodic amplified direct ophthalmoscopy check-up is identified as the most appropriate approach in screening for the universal population at risk. However, this method lacks direct sensitivity in direct ophthalmoscopy. In the contemporary world, newer methods of detecting and managing retinopathy are continuously being identified [8]. Early screening of the disease could enhance effective prognosis of growing retinopathy thereby reducing the rate of progress towards blindness. DR can be treated through vitrectomy and laser surgery. Despite the discovery of these advanced treatments, blindness from retinopathy cannot be restored. Therefore, early detection needs to be prioritized as a means to prevent loss of vision [9]. The published methods in [10] indicate that MAs could only be detected on fluorescein angiograms or through colour images. In these methods, the retinal features could be clearly distinguished from the Micro aneurysms (MAs). Fluorescein angiogram images worked better than digital colour photographs by providing contrast between the background and the micro aneurysms. However due to the 1:222,000 mortality rate for fluorescein angiograms accompanying the intravenous administration of fluorescein, the technique could not be used for purposes of large-scale screening.

1.5 Research Objectives

Propose a method to make the overall system for detection of MAs more robust.

1.6 Layout of Research work

Chapter 2 reviews existing MA detection schemes and describes the literature survey Detection of Micro-Aneurysms in Images of Retina for The purpose of Early Diagnosis of Diabetic Retinopathy.

Chapter 3 describes the design and implementation of the proposed MA detection method the chapter explains the tools used to implement the scheme. The screen shots of the implemented scheme are also given along with explanation in the chapter.

Chapter 4 discusses the results of the performance evaluation of MA using different image pixels.

Finally, in Chapter 5, the results obtained have been summarized and some of the future research directions and recommendations have been highlighted.

Chapter 2

Background and Literature Review

2.1. Overview

This chapter highlights the broad analysis of related literature that forms a solid base and highlights the necessity for this area of research. The chapter begins with the review of existing MA detection schemes and further examines the literature.

2.2 Review of existing MA detection schemes

Several systems have been developed for detecting MAs for the purpose of recognition of healthy and unhealthy patient's eye. Each system achieves a certain trade-off between robustness and accuracy for a given perceptual transparency. The choice of the system depends on several factors, most important of which are, pixels quality, the computational complexity of the algorithm and the application, which defines the degree of robustness required.

Detail descriptions of some of the popular MAs detection system and the steps involved in implementing are discussed.

They are mainly classified into two categories:

- Morphology methods
- Non Morphology methods

Morphology methods helps the researcher to unfold the complex and estimated issue. These methods are studied and modelled by breaking the system into two categories, first the major component of study is being separated, and then the methodology is being modelled and design to make the whole method more reliable. The drawback of morphological methods is the utilization of bigger structured elements which sometimes lead to wrong detection. Of course, non- morphology methods may be useful as copyright verification of results produced at the end. Non- morphology is based on mathematical modelling of the system with results having less errors.

The principles of detecting MAs can be defined as a flowchart as shown in figure 2.1. In the first step, the image is being pre-processed. The image pre-processing further helps to improve the inspection of system and hence more visible outcomes can be seen.

Because of photographic conditions, difference in fundus image has been developed. MAs can be incomparable viewed with green color the most hence RGB color is transformed into green-channelled images. Finally, a data set is created with images of different sizes, Images were enlarged from the smaller sizes using a bicubic convolution method by maintaining aspect ratio of each image and using the standard filters.

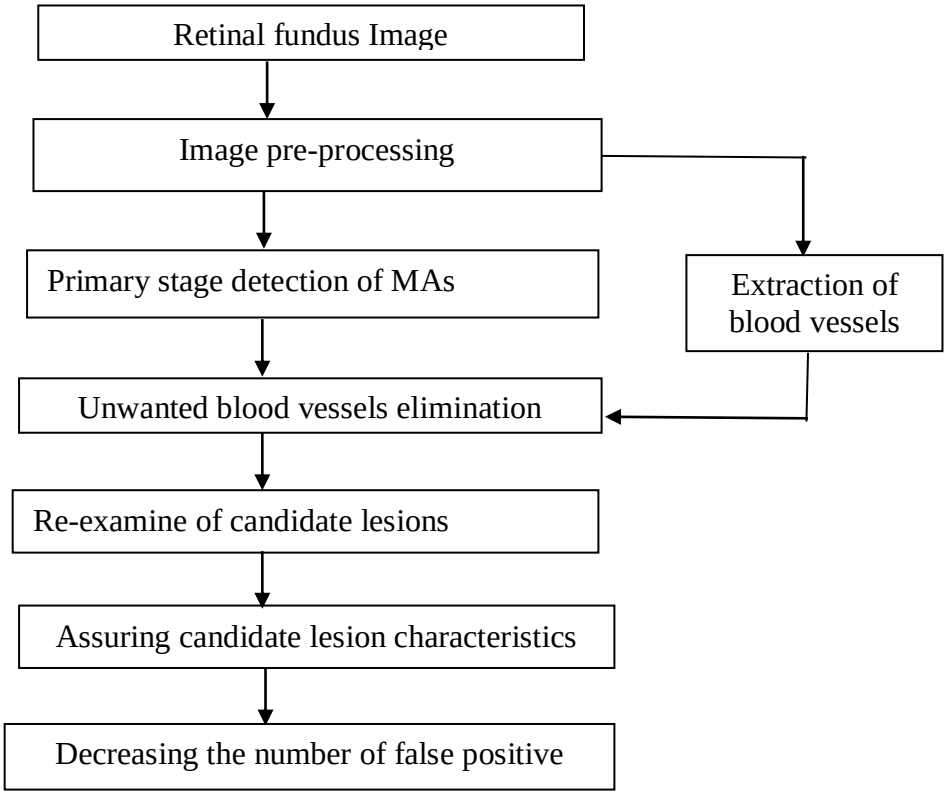

Figure 2.1 steps for detection of MAs [7],[22]

In the second step, detection of MAs is seen as lesions (a region in an organ or tissue which has suffered damage through injury or disease) which are darker than the surrounding regions. Hence they are easy to detect.

In the third step, the number of false positive detections are reduced. In order to eliminate the false positives, various methods have been followed by either morphological or non-morphological methods. Lesions present in blood vessel region as false positives are removed from the data list.

After the detection of false positives, the next challenge is the disturbance in the shapes of finally collected data. In the previous step, as certain methods were applied for the correct detection of false positives having adverse effect on image feature analysis, consequently re-examination of data lesion is made in fourth step.

As the initial detection leads to many false positives, thus a 12 image feature were calculated for each lesion. In this step of calculating 12-feature set, it includes two features each of:

a) Area.
b) Degree of circularity.
c) Size ratio in terms of length and width
d) Mean value of resulted lesion for each color bits.
e) Distinguishing among maximum and minimum picture (pixel)
f) Difference between mean values of data sets region and surrounding region.

For better performance, the authors suggested an approach of CAD is applied to detect MAs in retinal images. The approach used by author is "multi-scale correlation filtering" (MSCF) and threshold strategy which is a dynamic type i.e. changed according to the system requirements for intensity-based detection and localization of MAs in retinal images in a systematic structure [7], [22]. They define their model in two parts, in the first part which is the base of the model with vital information, we detect raw MAs using MSCF. In the later part (fine level) as defined by author, they classify true MAs by dragging out the 31 features from the level one candidates which are used to classify them.

2.3 Literature Survey

Lay [1983] et al. [7] presented a segmentation approach for retinal MAs for the calculating the retinal image problems using morphological methods. It leads to an image in the result in which using some threshold points. Whatsoever be the threshold point image recommended the structures smaller than that is not considered. Hence the difference of created image and the original image (it is for top-hat transformation) can be differentiated and helps to obtain MA. This is the approach forms the backbone of the research.

L.Vincet [1992] et al. [20] proposed other morphological operators which are applied to data with the steps having the extraction of image first and then in the second step classification process is followed.

T.Spenecer [1996] et al. [13] describes a new strategy for image-processing which not only find the presence of Mas in retinal images but also measures them using digital fluorescein angiograms. The first step of pre-processing is same as mentioned in

previous paper. Further for the initial segmentation, improved accuracy is achieved using matching filters and bilinear top-hat transformation. By giving the threshold point's candidate MAs is viewed in the output. A novel region-growing algorithm proposed by the author gives the output as a figure which observes the size, shape, and energy characteristics of individual candidate which can sought out the image in terms of the final segmentation of MAs. The technique presented in this paper follows the comparison of standard data with number of MAs laid down by five ophthalmologists, by following the procedures of Receiver Operating Characteristic (ROC) curves. This technique leads a new way in more reliable and accurate detection of DR.

M.J. Cree [1997] et al. [14] came out with the advanced version of digital image processing system, which provides motivation for developing more models and strategy to quantify MAs in digital fluorescein angiograms. In his paper the author talks about the automated computer processing where they mention about the admission of matching- eye retinal images for serial studies, eliminating the unwanted regions. Thus a new direction in research came out with the detection of MAs. According to the methodology proposed, the MAs detector was tested on a datasheet of 68 images collected from the patients suffering from diabetes containing 394 true MAs, these sets of data were generated after deep observation by an expert in the field. The MA detector achieved 82% sensitivity with 2.0 false-positives per image. A random generated test set, comprising 20 images resulting in 297 true MAs, was used to compare the MA detector with clinicians. The author results showed that MA detector provided the

"sensitivity of 82% for 5.7 false-positives" per image, while the clinician receiver-operator-characteristic (ROC) curve gives 3.2 false-positives per image at a "sensitivity of 82%". Hence the conclusion is drawn as the computer system can practically more accurately detect MAs. The benefits of using the dummy sets created by computer include good direction in the field, dynamic, speed and fully digitized.

A.J. Frame [1998] et al. [15] authors compared the performance of above mentioned computerized define classification steps for detecting MAs on digital angiographic images of the retina. Quantitation process based on approximation was not used till that time in clinical practice due to the large inner and outer observer variability. They were able to develop a full automated image processing system which could segment candidate objects (MAs or spurious objects) directly from the digital images. In the further steps raw data is collected for examination of MAs. Author proposed to follow with the methodology of 1659 candidate to skilled each classifier, set of 1067

candidates as independent set was used for experiment. He suggested a rule based system, which has a quantitative and logical rules, with linear discriminant analysis and a learning vector quantized artificial neural network methods. Each of them then analysed as useful data or spurious data. Useful data or MAs then directly extracted for digital images. ROC analysis helps to make surety about the data. Hence the conclusion has been drawn a higher performance at the output as compared to conventional methods.

A.Mendonca [1999] et al. [16] shows a technique for the automatic segmentation and counting of MAs in retinal angiograms of diabetic patients was obtainable. The criteria used to demonstrate a good capability and to differentiate MAs from other similar retinal structures. This combination technique helps in comparing the performance of computerized images which helps in temporal progression of DR and gives new loop-holes of the system.

An efficient algorithm for vessel-like pattern detection has been presented in Zana [2001] et al. [12]. For demonstrating a wide range of retinal images it is important to focus on robustness and accuracy of different images. The authors conclude with the comparison of performance evaluation that the complementarity of mathematical morphology and linear transforms helps in more reliable output. Further paper presents the vessels using shape properties, connectivity, as well as differential properties like curvature. It is the first step toward an automatic diagnosis software with some mentioned robustness and weakness which helps as a base for further study in this field. The limitation of the method is that its application is limited to eye fundus images.

J.Staal [2004] et al. [27] presented a method for automated segmentation of vessels in two-dimensional color images of the retina. The system definition was based on extraction of image ridges with vessel techniques which coincide with vessel centrelines. The ridges being considered as line elements. Further, the line elements partitioned the image into patches considering the image pixel as closest line element. For every line there was a local coordinate frame and its corresponding patch vectors are computed for individual pixels which can be classified using a k-NN-classifier and sequential forward characteristic selection. The algorithm was tested on a database having 40 manually images. The results showed that suggested technique achieves an area under the receiver operating characteristic curve of 0.952.

J. Lowell [2004] et al. [31] with the revolution in study towards obtain accurate dimensions of vascular widths, the authors present an algorithm to determine the vessel diameter to sub-pixel accuracy. More attention in this side was important

because of its vital and challenging process in automated retinal image analysis. In the algorithm, the diameter measurement is based on difference of Gaussian model, designed in such a way that it helped in improvement of designing of two-dimensional intensity vessel segment. The author then compared it with the performance of the method which is evaluated against that time existing algorithms and conclude the results from 100 sample profiles and his algorithm proved over 30% more precision than the compared techniques and is accurate to a third of a pixel which was appreciable.

M. Niemeijer [2005] et al. [18] had proposed a new approach of using digital color fundus photographs. The advantage of the model is its robust detection of red lesions. In this article author combined the work suggested by Spencer [1996] and Frame [1998] along with two more new approaches. Their first approach was to detect system based on pixel classification. Using this technique, vasculature and red lesions are separated from the background of the image (noise filtering). The leftover was considered possible red lesions. In addition to it, the detected candidate objects are classified a k-nearest neighbour (k-NN) classifier. Extensive evaluation was performed to verify it further more as if an image contains red lesions. The results show that the system had a sensitivity and specificity of 100% and 87% respectively. The method is compared with a number of different automatic systems and the algorithm performs best and give true positives output of observing the presence of red lesions in the images.

A.D. Fleming [2006] et al. [17] defines a problem of detecting the MAs and other dots that occur on the retina. They suggested a scalable approach of self-regulating the MA detection using image contrast normalization. They suggested a method of watershed transform to differentiate between if there is no vessels or other lesions. Local vessel detection technique helps best for detection of dots within vessels. Concluded article shows the presence of individual MAs are detected with sensitivity and specificity 85.4% and 83.1%

T.Walter [2007] et al. [19] leaded to the era of in computer-assisted diagnosis of DR. It addressed the automatic detection of MAs in color fundus images. Computer-aided diagnosis (CAD) could effectively use by physicians and ophthalmologists in detecting the lesions in mass screening. The author notes that the methods described had highly competitive status according to the online competitions held to assess the performance levels of the methods. In grading DR, the micro aneurysms significantly guide the ophthalmologists on whether the eye of the patient can be regarded healthy or not.

For this reason, extensive studies on creating a computer aided diagnostic (CAD) system for detecting DR and analysis of retinal images have been conducted widely. The algorithm automatically differentiates between real MA and other objects. The author choses the classification performance based on the on kernel density estimation with variable bandwidth. A database of 21 already defined images has utilized to skill and feed the algorithm. Results shown that by comparing the algorithm are as shown in table as follows:

Sensitivity	88.5%
Average number of false positives	94 images

Table 2.1 kernel density estimation result [30]

E. Ricci [2007] et al. [29] upgrades the earlier approaches of thresholding and two segmentation methods. In the first approach, using thresholding the basic line detectors unsupervised pixel classification is obtained. A feature vector then constructed for supervised classification which is sought out by support vector machine. The results are obtained using receiver operating characteristic analysis shows the effectiveness of the system.

A. Mizutani [2008] et al. [23] investigated a "computerized method for the detection of MAs on retinal fundus images, which were obtained from the Retinopathy Online Challenge (ROC) database". ROC was a new beginning of efficiently finding the MAs in retinal image. ROC method depends upon the presence of gold standard locations which defined it as an infected one or the healthy one. The ROC comprises of 50 training cases, with the presence of gold standard locations of MAs being defined and 50 test cases without the gold standard locations. These equal proportions of the ROC is applied to twelve image features standard as given by experts of the area, and hence candidate lesions were classified into pure or impure images. For further defining the accuracy of the system rule-based method and an artificial neural network had been applied. The results showed that the "true positive fraction was 0.45 at 27 false positives per image. 42 percent of MAs in the 50 training cases were considered invisible by two algorithms". The sensitivity was measured of 65% at 27 false positives per image for 50 visible test-beds.

G.Quellec [2008] et al. [26] Presented an automatic method to detect MAs in retina photographs. MAs are the first stage appeared as a symptoms of DR. If it is detected in the early stage, prevention measures could be used to avoid the severe complications. Automating this task, produce the new revolution with accuracy. Genetic algorithms

help in optimizing the process followed by Powell's direction set descent. For calculating the results authors evaluated on 120 retinal images data analysed by an expert. The author uses the optimal wavelet and performance evaluation of the proposed is being compared with all the conventional wavelets. The images are classified as three different modalities: color photographs, green filtered photographs and angiographs. Table 2.1 shows the sensitivity and positive predictive values as given in the article which is better than previously published methods.

Modalities	Sensitivity	positive predictive value
color photographs	89.62%	89.50%,
green filtered photographs	90.24%	89.75%
angiographs	93.74%	91.67%,

Table 2.2 comparison of Three Modalities

C.I. Sanchez [2009] et al. [25] Analysed the problem from different angle based on "mixture model-based clustering and logistic regression" which effectively detects the presence of MAs in the retinal images using binary methods. The method is computed by considering the public database given by the expertise in the field and is an open access as proposed by the Retinal Online Challenge in order to obtain an objective better results and further study with advanced level algorithms.

B. Zhang [2010] et al. [22] presented a new approach with the collaboration of multi-scale correlation filtering (MSCF) and dynamic thresholding is developed. The method consists of two steps: MA candidate detection is the basic detection or unsupervised extraction and true MA classification (final detection with true results). The approach was based on ROC selection. The scales selection in the first level is essential to the success of succeeding steps. Sigma values are selected in a way that K-NN of different sizes always produce a high correlation coefficient. More significantly, images in DIARETDB1 database were acquired which is an open access and the data here is provided by experts and clinicians, which provides a general platform to benchmark different algorithms for the detection of MAs.

T.Zhu [2010] et al. [28] proposed the cross sectional profiles for defining the retinography issues along with the introduction of symmetry and asymmetry Fourier transformation. Phase congruency is utilized as it is invariant to vessel brightness. Results were obtained to show the efficiency of the proposed algorithm technique by implementing it on fluorescein images and color fundus images. The author promised the new algorithm technique as good for automated vessel detection and less complex further the results preservation for further analysis adds the more advantage to the articles pocket.

L.Giancardo [2011] et al. [30] the MA detection method proposed by the author is based on Random transformation with similar cross- sectional theoretical background as given by [30]. The author proposes a 2D" tramline" filter for the better accuracy of detection.

I.Lazar [2011] et al. [26] Authors presented a method that is capable calculating infected image without the use of supervised learning technique. The author uses the simple approach of thresholding and binary logics to get the true positive output of MAs. The author talks about the probability score method, in which the MAs area are being considered as high score areas while the other one is the minimal score area. The probability and binary output is thresholded to particular value and hence final MAs are calculated. Data being taken as input is the open access public data standardized by the experts. The author believed it to be the best method based on ensemble based-algorithm and holds the first place in the mentioned online competition.

K. Ram [2011] et al. [21] has formulated MA detection as a target detection in clutter problem and proposed a successive clutter rejection solution for MA detection. The method is based on the frequency occurrence and discriminability. Morphological methods as described above had been mentioned in the paper. The target detection and clutter rejection strategy helps in giving the cascading solutions thus the early stage of the process at least gives the good coarse level results which makes the final step bit simpler. Results obtained are having visible good effect at the output as comparing with the existing algorithms. The results put a visible effect in the performance across datasets and also discuss about the difficulties that could cause problems in candidate selection due to the variability found across datasets.

Istvan [2013] et al. [32] proposed a method for detection of micro aneurysms in retinal images. Peak detection methods were used to detect positive monotone ramps of the profile. The ramps can either be positive/ increasing or negative/ decreasing. In this analysis, only the maximum regions qualified to be candidates.

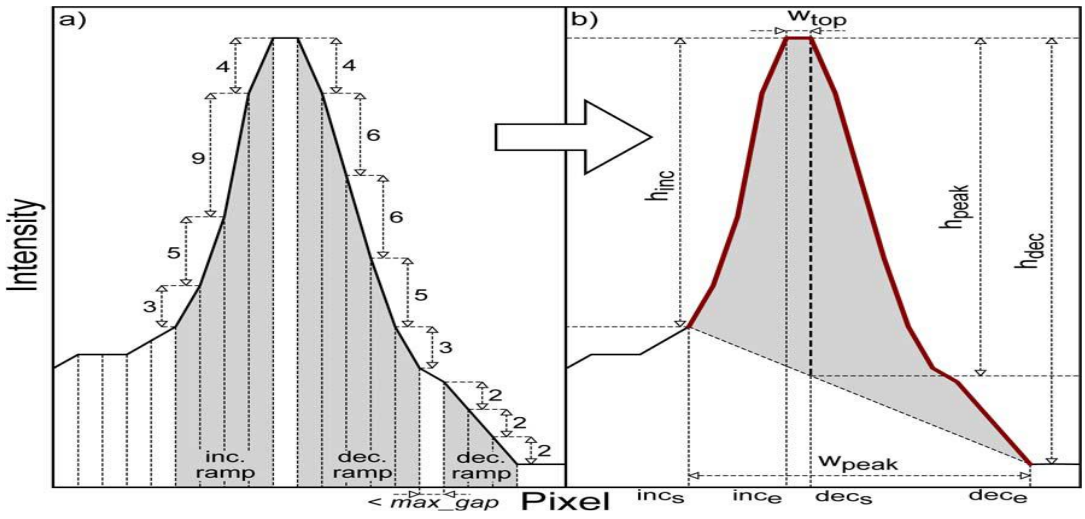

Figure 2.2 Rising and declining ramps on a sample profile. Figure 2.3 The outcome of the peak exposure and the tabulated peak measures.

With the peak detected at the center of the profile, various properties can be calculated. For instance, the variation between the initial and final indices of the peak forms the peak width. The top width can be calculated by determining the scope of the gap between the rising and declining ramp. Also, the increasing ramp height, the decreasing ramp height, the increasing ramp slope, the decreasing ramp slope and the increasing ramp height can be calculated. Values of the peak width relate to the extrapolation of the figure in particular consideration. Alternatively, the scope of the structure can be determined by the values of top width. Also, the slopes and heights of the rising and falling ramps provide information on the surroundings as well as the sharpness of the transition in image intensity. The peak height values can be used to calculate central pixels on the baseline

The study in [32] was based on the concept of examining directional cross-sectional profiles. Characteristically, the profiles arise from the candidate pixels of the pre-processed image. The authors applied peak detection for each profile. They further calculated the values describing the height, shape and size of the central peak. Statistical measures from the cross-sectional changes of orientation constitute the feature set for identifying false candidates. Statistical measures obtained from the cross-section orientations identify relevant feature set for eliminating false candidates. Based on the final score the remaining candidates feature values can be obtained. This method successfully passed through the Retinopathy Online Challenge and scored higher than previous methods. The authors explain about the “Retinopathy Online Challenge is an international online competition” which is well renowned for the precise detection of

MAs by comparing it with others under the same conditions." The open access dataset consists of "50 training and 50 test images called as gold locations", but the location of the MAs is only available for the test set. Hence each image gets an opportunity to participate in the test sets. The results are obtained as candidate coordinates and confidence values. At the end, sensitivity defines the output of ROC result the propose method has been made as per two classifications: first is to make the set of positive MAs and second is the set of negative MAs which is done manually. The process is accomplish using Bayes classifier. Decision of classifier is made depending on the parameters such as robustness, and speed. The author has claimed to achieve the overall score of 0.423when being evaluated by ROC which is considered as an appreciable value. It achieves the higher sensitivity at low false positive rates. FROC curves (free-response receiver operating characteristic) achieved the score of 0.3548

2.4 Summary

The paper by Istvan Lazar [2013] provides a modern and evolved method for detecting MA. The paper subsumes many of the papers reviewed above in that it avoids many of the pitfalls of previous papers. However, the paper has a shortcoming that may prevent the best possible detection performance. In evaluating local candidate MA, the authors use an ad hoc method to measure local changes of slopes of lines radiating from a local maximum as mentioned above in literature review. In this thesis, an attempt is made to improve this aspect of the approach. Instead of an ad hoc method, a method is presented based on robust mathematical description of the candidate MA.

CHAPTER 3
METHODOLOGY

3.1 Data

Detection of retinopathy in its early stage represents one of the major problems recently facing the current medical industry for an effective design of high performance MAs algorithm. On the other hand, they provide a comparison of results, which is useful for the verification of performance metrics. The chapter presents important MAs metrics. The evaluation criteria known from literature analysis are introduced and described. The presented strategy is used for examining the following chapters of this research work.

Before discussing the performance evaluation criteria, we have to define DIARETDB1 - Standard DR Database. It is an open access database comprises of "89 colour fundus images of which 84 contain at least second stage of retinopathy signs (MAs) of the DR", and 5 are perfect images of normal eyesight 6/6 participated in the evaluation. 50-degree field-of-view digital fundus camera are used for the purpose of accurate capturing of Images with either same or varying imaging settings. The data information is given by the experts who are being advised by certain parameters while they design the data sets. By following the parameters and protocols the data is made known as DIARETDBI. [33]. this data set is called as "calibration level 1 fundus images".

3.1.1 Ground Truth

Results are being considered from 4 experts' research outputs by using a software tool provided for image annotation. An expert is said to be a person with deep knowledge and experience in ophthalmology. These experienced people then mark the areas related to the MAs, haemorrhages, and hard and soft exudates. The expert's works on protocols of considering only the area which is the part of study and does not mislead the study by considering the unwanted regions of retina. Further they need to prove the ability of maximum positive results and define the "single most representative point for each finding". The definition set by them are, [<50 %, ~>50%, ~100%], representing the "certainty of the decision that a marked finding is correct".

This is important as the uninstructed dataset leads to the considerable differences between the observers in the same field. Therefore, special care is taken with expert advice and best of their knowledge for a better spatial accuracy and suppression of outliers [33]. It can be seen as shown in figure 3.1

Figure3.1 (a) For experiment image

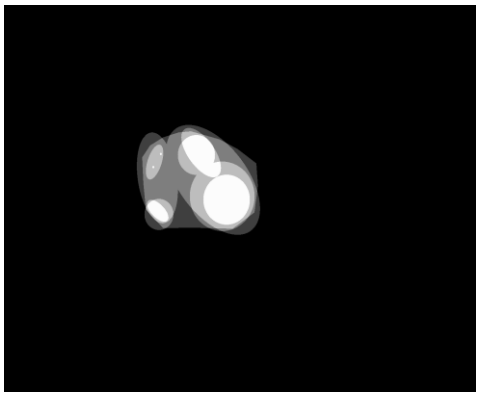

Figure3.1 (b) hard exudates

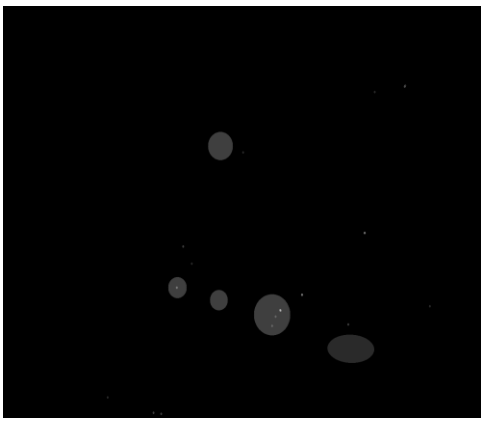

Figure 3.1(c) Microaneurysms

3.2 Processing Steps

Keeping in view a comprehensive set of relating to MAs detection, the performance metrics listed below have been reported in this research work to assess the performance of MAs detection: The simulation tool used for this study is MATLAB:

The algorithm can be evaluated using three basic steps:

- Image Pre-Processing
- Local Maximum Extraction
- Determination of coefficient Gaussian Model
- Selecting the local maximum peak
- Fast Fourier Transform of the Coefficients
- Classification

3.2.1 Image Pre-Processing

All the steps of pre-processing algorithm were followed as per published work of Lazar & Hajdu (2013). The green channel of the input image was extracted as it retains most of the image information. The extracted green channel was normalized to stretch the dynamic range of the greyscale from 0 to 1 (as the input image is 8-bit unsigned integer from range 0 to 255). Then green component of the image was inverted. In the resulting inverted image micro-aneurysms, haemorrhages and veins appear as bright structure. This means that these structures will be of high intensity compared to the background. A low pass filter was applied to smooth the image noise. The low pass filter used was a Gaussian Low pass filter of mask size 85 and variance 1 pixel. After smoothing the image and removing the noise, the image clarity is improved.

3.2.2 Local Maximum Extraction

After the pre-processing step, the next step was to extract the local maxima in the pre-processed image. The MAs have structure similar to a Gaussian distribution about at least one local peak (or more). The highest value of each 3 x 3 square was recorded. The location was recorded only if the maximum value of the square was at the centre. The local maximum in this case compares a pixel with the 8 pixels in the 3x3 neighbourhood and if the pixel has equal or larger values compared to the other 8 pixels, then the pixel is a local maximum. These local maxima are possible candidates for the MAs.

3.2.3 Determination of the coefficients for Gaussian model

The MAs have structure similar to a Gaussian distribution about at least one local peak. A local patch of size 15 x 15 was centred on each local maximum. The following model was fit to each such patch. The model is shown below.

$$H(r,\theta) = He^{-\lambda(\theta)r^2} \quad \text{....3.1}$$

The coefficients in the exponent $\lambda(\theta)$ are a function of the angle θ. The angle is a continuous function from 0 to 2π radians. The angle is discretized in 16 different angles as

$$\theta = 0, \frac{2\pi}{16}, \frac{4\pi}{16}, \frac{6\pi}{16}, \ldots\ldots, \frac{30\pi}{16} \quad \text{....3.2}$$

Hence first the interpolated pixel positions are calculated using cubic interpolation and then the angle $\lambda(\theta)$ is calculated.

Let the local maximum be H then we define

$$h = \ln(H) \quad \text{....3.3}$$

At a given orientation angle θ, let the positions be r_i. As the pixels are discrete, so the positions of pixels for a neighbourhood of 15x15 (the centre pixel and a neighbourhood consisting of 7 pixels to the right of pixel, 7 to left, 7 above and 7 below) can be used for r_i i.e.

$$r_i = i \quad where\ i = 0,1,2,3,4, \ldots 7 \quad \text{....3.4}$$

The interpolated pixel positions for a centre pixel at (r, c) and orientation angle θ:

$$x_i = r + i\cos(\theta) \quad \text{...3.5}$$

$$y_i = r + i\sin(\theta) \quad \text{....3.6}$$

Using cubic interpolation on the image pixel values p(x, y), the pixel intensity values $p_i(x_i, y_i)$ are calculated. Then defining

$$z_i = \ln\big(p_i(x_i, y_i)\big) \quad \text{...3.7}$$

The coefficient $\lambda(\theta)$ for that particular angle orientation θ can be determined as:

$$\lambda(\theta) = \frac{h\sum_i r_i^2 - \sum_i z_i r_i^2}{\sum_i r_i^4} \quad \text{...3.8}$$

3.2.4 Selecting the Local Maximum Peak

The local maxima may not be unique. For example, there may be several peaks. The number of peaks in the local neighbourhood is required to be reduced and the overall local maximum is found to represent the local neighbourhood. There are two ways to approach this problem. During the training phase, the human expert results are known. The local maximum peak that represents the candidate MA can be chosen by finding the nearest peak (in Euclidean distance terms) from the candidate MA position given by expert. The other technique is to find the local maximum in the same neighbourhood in the green component of the image fundus. The local maximum in the binary image that is nearest (in Euclidean distance terms) to the local maximum in the green component is chosen. The second technique was implemented in this study.

3.2.5 Fast Fourier Transform of the Coefficients

The values of the $\lambda(\theta)$ for different θ_k at each local maximum are saved in a matrix. Each row of the matrix represents a different local maximum. The matrix has 16 columns which represents the coefficient value at each angle. The Fast Fourier Transform (FFT) of the matrix is taken for each row independently as 1-D vectors. The magnitude of each Fourier coefficient is calculated. As magnitude of FFT is symmetric and even function, so the 16 point FFT results in eight distinct coefficients (including digital frequencies 0 to π). The remaining coefficients are for digital frequencies ($-\pi$ to 0) and are not used due to symmetry.

3.2.6 Classification

From the human expert opinions, the positions of the true MAs were identified. The true MAs had divided in two types (red dots and non-red dot haemorrhages). The number of candidate MAs were divided in two lists roughly evenly. The two sub lists are created by randomly selecting MAs such that half the red and non-red dot haemorrhages were in one sub list and the other half were in the other sub list. Although measures were taken to divide the true MAs (red or non-red) in half, but it was ensured that the division is random so that there was no bias in the results.

From the index sub lists created above, two data sets were generated. One sub list was chosen as the training data and the other sub list is chosen as testing data. The magnitude of FFT (8 coefficients) was stored in the matrix from the last section and the data was

divided into two parts such that the 8 classification parameters of half the true and candidate MAs were in one list and the other half are in the other list.

As the expert opinions were known, the group data can be generated. The data was divided into three classification groups. One classification group are those data points that correspond to non-MAs. The second group are true MAs of red dot type. The third group are true MAs of non-red dot type. To achieve this (dividing the group data into three classification groups), two column vectors were appended to the data. If any index (row) of the data was the FFT magnitude coefficients of the non-MAs, then the appended vector at that index is binary '00'. If any index (row) of the data is the FFT magnitude coefficients of the red dot MAs, then the appended vector at that index is binary '11'. If any index (row) of the data was the FFT magnitude coefficients of the non-red dot MAs, then the appended vector at that index is binary '10'

The training and test data (which represents the 8 parameters extracted from the magnitude of FFT) is applied to a Discriminant Classifier. The classifier returns the predicted results by classifying the test data based on the classification parameters and the known pattern of the training data. The results of the classification are evaluated as following:

- True Positive: A candidate MA in the test is true MA and is classified as a true MA by the classifier.
- True Negative: A candidate MA in the test is not an MA and is classified as not an MA by the classifier.
- False Positive: A candidate MA in the test is not an MA and is classified as a MA by the classifier.
- False Negative: A candidate MA in the test is a true MA and is classified as not an MA by the classifier.

The fundus image is shown below in figure 3.2.

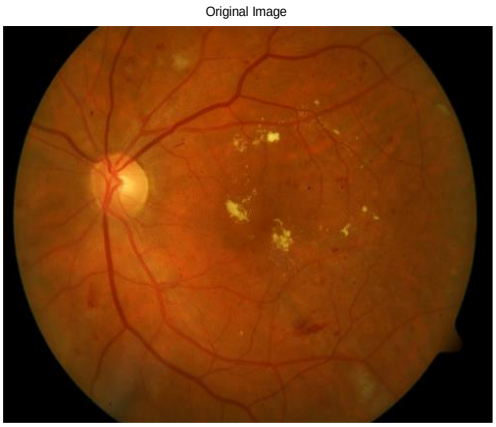

Figure 3.2: RGB retinal image fundus

The green component is extracted from the image fundus shown in figure 3.3 below. The image fundus is an RGB image while the green component image is greyscale as it only has one component. The green image may not stretch across the full dynamic range (which is 0 to 255 greyscale for 8-bit green component).

Figure 3.3: Green Component extracted from RGB image fundus

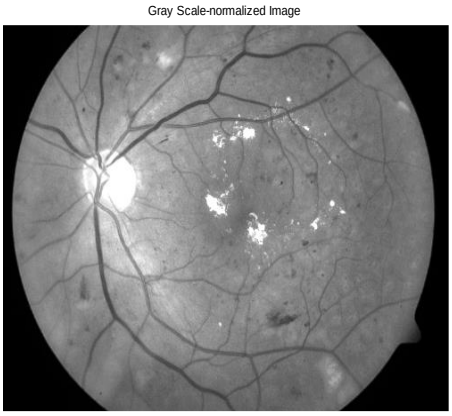

Figure 3.4: greyscale normalized image

The green components image is normalized so that the dynamic range stretches from 0 to 255. The image is then reversed in grey scale (i.e. the white 255 is converted to 0 and 0 is converted to 255) as shown in figure 3.5.

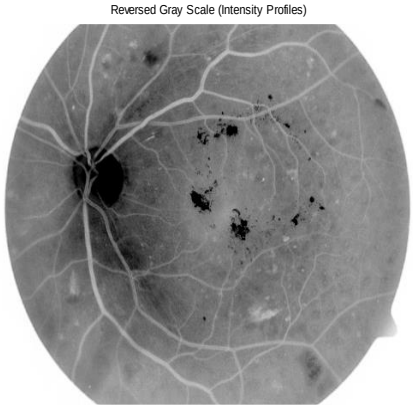

Figure 3.5: greyscale reversed image

A Gaussian filter is applied on the image to remove the background noise during image acquisition as shown in figure 3.6.

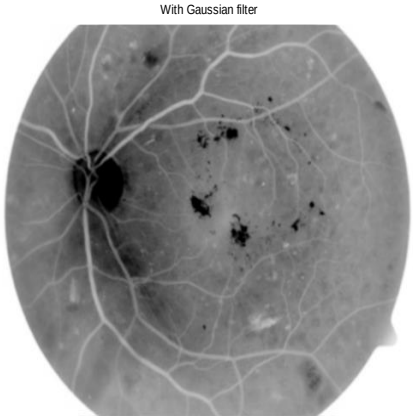

Figure 3.6: After applying the Gaussian filter

The greyscale inversion results in the background shown in black in figure 1 to be converted to white. The image pre-processing is completed by converting the background back to black as shown in figure 3.7.

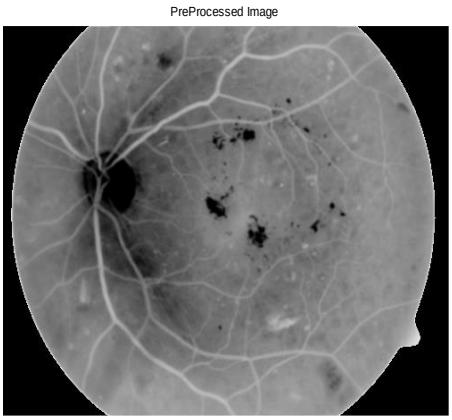

Figure 3.7: Pre-processed image

On the pre-processed image, the local maxima are extracted using a 3x3 rectangular neighbourhood. The local maxima are shown in figure 3.8. There are 4098 total local maxima in the figure3.8.

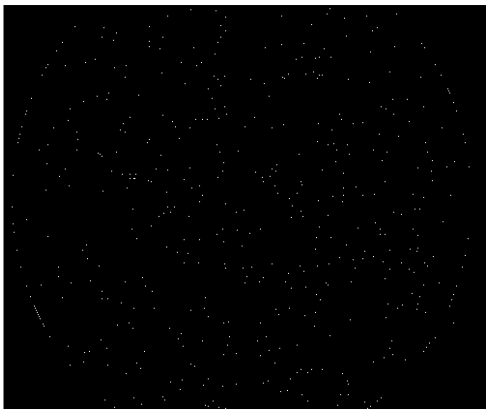

Figure 3.8: Local maximum extraction

For each of the 4098 local maxima, a coefficients were calculated by using 15x15 local neighbourhoods on 16 angles from 0 to 2π and are stored in the matrix. This results in 4098 x 16 matrix of coefficients. The 4098 rows represent the number of local maxima extracted and the 16 columns are the coefficients of the coefficients at the 16 angles. The coefficients $\lambda(\theta)$ are plotted for 3x3 (9 point) neighbourhood in figure 8. The image shows the coefficient for angle 0 to 2π for local maximum at subplot element (2, 3)

which is the middle subplot. The other 8 subplots show the coefficients at the eight pixels around the local maximum.

3.2.7 Analytic results in ideal cases

For simple ideal candidate MA, it is possible to compute λ(θ) directly.

- **Ideal true MA**

If a true MA has a Gaussian signature in the image of height 1 and then the image may described by the function

$$I(r,\theta) = e^{-r^2} \qquad \ldots 3.10$$

In this case the model G(r,θ) fit exactly with λ = 1 for all θ (Figure 3.9). The Fourier transform of λ is zero except the DC component (Figure 3.10).

- **Ridge formed by a vessel**

A blood vessel in the image appears as ridge. If the cross sections of the vessel is a Gaussian, then the appearance of the vessel in the image may be given by the function.

$$I(r,\theta) = e^{-r^2}\sin 2\theta \qquad \ldots 3.11$$

By inspection,

$$\lambda(\theta) = \sin 2\theta = 1/2 - 1/2\cos 2\theta \qquad \ldots 3.12$$

Thus the Fourier transform has value 2 in the DC component at 2 Hz (Figure 3.10).

- **Intersection of two vessels**

The crossing of two vessels is sometimes detected incorrectly as a MA (Figure 1). If two vessels are perpendicular and cross sections of the vessels are Gaussians, then an example of such an intersection may be given by

$$I(r,\theta) = e^{-r^2\cos^2\theta} + e^{-r^2\sin^2\theta} \qquad \ldots 3.13$$

In this case, the model is G(r,θ) = $2e^{-\lambda r^2}$ since the height of the candidate MA is 2. The function λ(θ) cannot be determined by inspection alone. Following the suggested regression strategy above, for a fixed direction θ, the objective is to find λ to minimise

$$E(\lambda) = \prod \ln(I(r,\theta) - \ln(G(r,\theta)\prod^2 = \int_0^R [\ln(e^{-r^2\cos^2\theta} + e^{-r^2\sin^2\theta}) - \ln(2) + \lambda r^2]^2 dr. \quad \ldots 3.14$$

Differentiating with respect to λ and setting the result to zero gives

$$0 = \frac{dE}{d\lambda} = 2\int_0^R [\ln(e^{-r^2\cos^2\theta} + e^{-r^2\sin^2\theta}) - \ln(2) + \lambda r^2]^2 dr \quad \text{....3.15}$$

And so

$$0 = \int_0^R r^2 \ln(e^{-r^2\cos^2\theta} + e^{-r^2\sin^2\theta})dr - \frac{\ln(2)R^3}{3} - \lambda\frac{R^5}{5} \quad \text{....3.16}$$

Solving for λ gives

$$\lambda(\theta) = \frac{5}{R^5}[\frac{\ln(2)R^3}{3} - \int_0^R r^2 \ln(e^{-r^2\cos^2\theta} + e^{-r^2\sin^2\theta})dr \quad \text{...3.17}$$

Note that the derivation above is not specific to the particular surface I(r, θ). In general, the continuous analog of the regression above gives the formula for λ (θ) as

$$\lambda(\theta) = 5/R^5[\ln(I(0,0))R^3/3 - \int_0^R r^2 \ln(I(r,\theta)dr] \quad \text{...3.18}$$

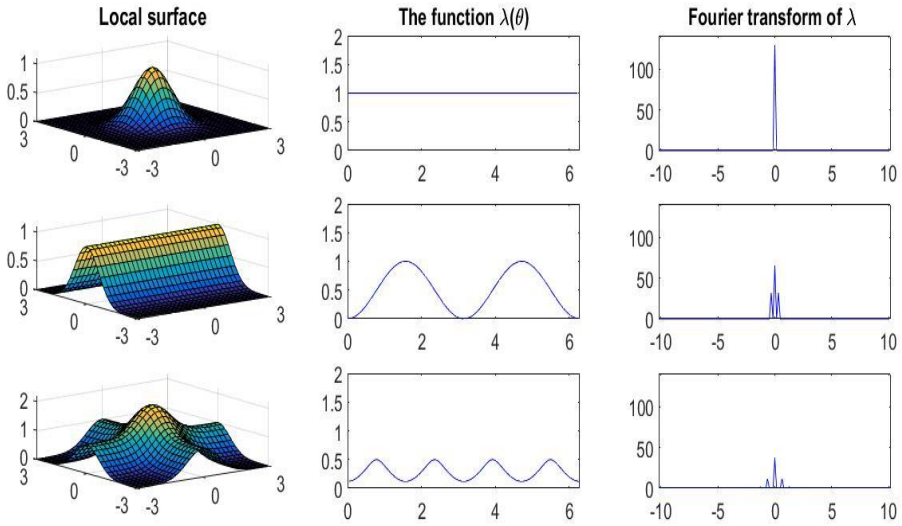

Figure 3.9 Three ideal image intensity surfaces, the associated functions λ(θ) and the Fourier transform of λ.

The first few normalised Fourier coefficients for λ associated with the three ideal image surfaces in Figure 3.9. For the first surface, λ(θ) = 1 and so the Fourier transform only has a response in the DC component. For the second surface,

$\lambda(\theta) = \frac{1}{2} - \frac{1}{2}\cos 2\theta$ and so the normalised magnitude response has value $\frac{1}{2}$ in the DC component and $\frac{1}{2}$ in at frequency 2 (frequencies are in cycles per 2π radians). However, only the positive frequency response is shown and so this carries a value of $\frac{1}{4}$. For the third surface, the intersection of two vessels, $\lambda(\theta)$ is more complicated but should have a response at frequency 4. The responses at multiples of 4 indicate period corrections to the fact that $\lambda(\theta)$ is not an exact sinusoid.

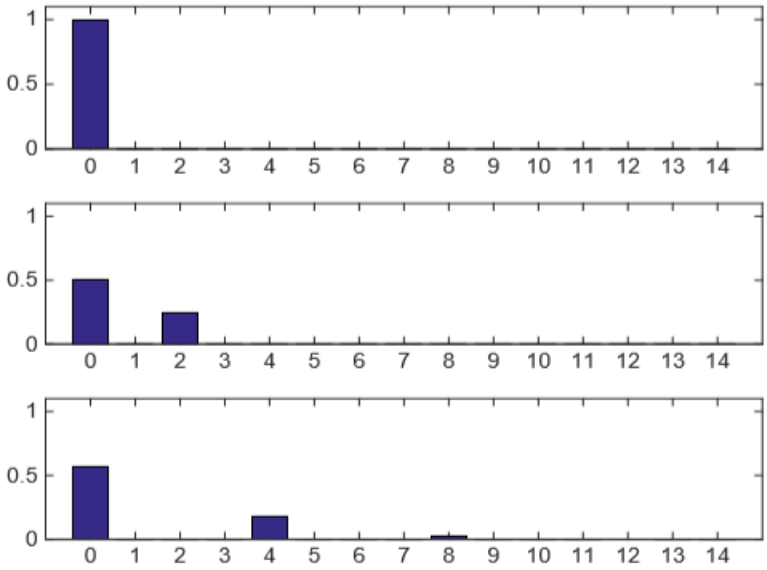

Figure 3.10 Graphical output The horizontal axis is in cycles per 2π radians

- **Finding the false positive in non-annotated images**

For finding the number of false positive for the rest of images which is not annotated by the experts needs to be focussed. Hence these non-annotations have been studied in our research and results have been drawn. As per the standard definition, we have a variety of positive (normal) and negative images. Our proposed strategy is to find the mean and the standard deviation of the number of false positive found by the algorithm to compare the differences between 3 normal images and 83 negative images to be tested by the method. These images have been taken from 89 image dataset which is an open access for analysing the results

.

3.3 Summary

This chapter identifies the various procedures which we follow for MAs detection, such as image pre-processing, local maximum extraction determination of the coefficient for Gaussian model, selection of local maximum peak, fast Fourier transform of the coefficients and classification of MAs to signal Processing. Finally, the chapter lists following principle steps that have been used in this research.

- Pre-processing of image is executed from the data set obtained as explained above.
- Extract the local maxima with mathematical morphological methods.
- We propose a formula to find the difference between true positives and false positives which is based on 12 feature values as being explained in literature. With the propose model we classify more efficiently between an image and ridge formed by a vessel.
- Re-examination is done by using Fourier transformation in the final step for the classification of local maxima as true positives.
- Non-annotated images have been analysed.

CHAPTER - 4

RESULTS & DISCUSSIONS

The results are collected by applying model to MAs for the detection of retinopathy in early stage. The criteria of performance evaluation will determine the reliability of the model.

4.1 screen shots of proposed model results

For each of the 4098 local maxima, a coefficients were calculated by using 15x15 local neighbourhoods on 16 angles from 0 to 2π and are stored in the matrix. This results in 4098 x 16 matrix of coefficients. The 4098 rows represent the number of local maxima extracted and the 16 columns are the coefficients of the coefficients at the 16 angles. The coefficients $\lambda(\theta)$ are plotted for 3x3 (9 point) neighbourhood in figure 8. The image shows the coefficient for angle 0 to 2π for local maximum at subplot element (2, 3) which is the middle subplot. The other 8 subplots show the coefficients at the eight pixels around the local maximum. Fig 4.1 shows coefficients plot against angle at the local maximum and the 8 points around the local maximum. The image tested here has a total of 32 true MAs. There are 21 MAs which are non-red dot MAs and 11 red dot MAs. The 4098x8 matrix is divided into two data sets of 2049x8 matrix each. The division is carried out in such a way that 11 non-red MAs and 6 red dot MAs in first data set (called the train data set) and the other data set contains 10 non-red MAs and 5 red dot MAs (called the test data set). The division is done randomly so that there is no bias. This means that only the number of true MAs in each data set is controlled but the MA that goes to each data set is chosen randomly.

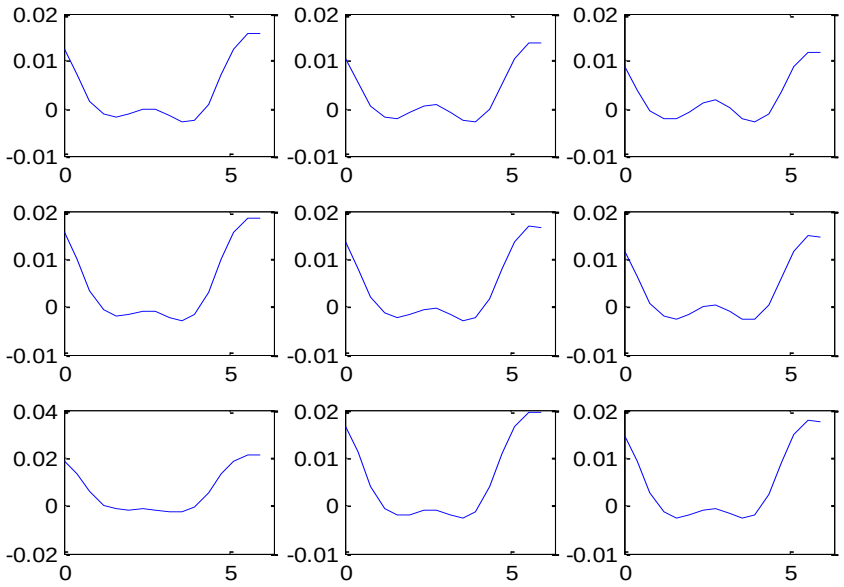

Figure 4.1 coefficients plot against angle at the local maximum and the 8 points around the local maximum

The position of the 32 true MAs are known from the expert opinions and a group classification is constructed from the known positions and the type (red or non-red dot haemorrhages). The training and testing data was applied to the classifier.

The main objective of this study is to be able to detect the red dot haemorrhages which are smaller and difficult to detect. As explained earlier, there are 5 red dot haemorrhages in the test data set. The results below show 4 out of 5 red dot haemorrhages are detected successfully by algorithm developed.

The method was trained on randomly selected 6 MAs and many non-MAs. It is tested on 5 MAs and many non-MAs from the same image. The classifier is trained by first image for which the expert opinions are known. The classifier can be then saved as a data set so that new images can be classified. The results show that 4 out of 5 been selected as true positives, which indicated that the methods will be useful. It should be tested on many images, but there was not an expert annotation for the other individual images.

Abnormal image (Testing image).		True labelled	
Detected		Positive	Negative
	Positive	4	604
	Negative	1	1438

Figure 4.2 Confusion matrix for abnormal fundus image

4.2 Results for non-annotated Images

	μ= Standard deviation± mean
Normal images (Positive images)	μ= 1856± 533
Abnormal images(negative images)	μ= 926± 480

Table 4.1 results of non-annotated images

The results show that 3 normal images has been obtained with the standard deviation of 1856 and the arithmetic mean is calculated as 532.69 which is round off taken as 533. We treat it as a true positive images. The rest 83 negative images have been calculated as a standard deviation of 926 and the arithmetic mean is calculated as 480. The result has been evaluated by taking the mean of position and height of the images.

4.3 Conclusion

The classification performed was able to detect 80% of all the MAs (red and non-red dot haemorrhages). The classification training data only contained 17 true MAs and 2049-17 = 2032 non MAs. The 17 true MAs are 11 non-red dot MAs and 6 red dot haemorrhages. The results can be improved further by using multiple images with known expert results so that the training data set can include a larger number of true MAs. Our observations reveal the difference of positive and negative non-annotated images. We have extracted the 3 best images (true positives) from the set of the non-annotated data with 90% of accuracy.

CHAPTER-5

SUMMARY AND FUTURE STUDY

5.1 Summary

In this research work, a technique for detecting MAs techniques has been studied and investigated. A novel MAs model is proposed in which determining the spot of MAs are quiet accurate and the overall system, is reliable. In the proposed scheme we modelled the intensity at candidate MA as the function. For a fixed local maximum and a fixed direction θ, regression is used to fit the function H(r, θ) to the image intensity values along the line in direction of θ. This results in a value for the parameter in every direction θ. For a fixed local maximum, the values of viewed as a function of θ characterise the local image intensity pattern. If the local intensity maximum is an isolated maximum, then the (θ) will be constant. If the local maximum is part of a ridge, then will be a small number in the direction of the ridge but a large number in the direction perpendicular to the ridges. If the local maximum is stems from the intersection of two blood vessels, then the function will show greater oscillation. By taking the Fourier transform of the function , the pattern of oscillation becomes rotation invariant. Thus local maxima are classified as a true MA or not based on the Fourier transform of . The simulation was done in MATLAB and the results has lead the retinopathy detection in new direction with improved reliability.

Our results show a clear difference between the numbers of the false positive in positive images and negative images. Thus, the proposed method works but to some extent. Thus, more data sets required to test the method on.

5.2 Future Study

Today there is much interest in detection of retinopathy so as to stop spreading it widely in diabetic persons. Currently, the algorithm for automatic detecting micro aneurysms does indeed find MAs but also reports some false positives - meaning that some spots are identified as micro aneurysms that were not annotated as locations of true micro aneurysms. This is not unexpected at this stage and further work will be required to understand the reason for the false detections and then take action to mitigate this problem. Probably, this step will have to part of a future project

Therefore, more research will be needed in the future. The study may be carried on in future with following direction:

1. What is the distribution of micro aneurysms in normal people? In other words, is it normal to have one or two micro aneurysms or does normal mean that there are no micro aneurysms at all?
2. Its results are preliminary and will be improved. This makes a difference in how we evaluate the performance of the algorithm.
3. Work needs to concentrate more on reducing false positives.

REFERENCES

1. Kertes PJ, Johnson TM, eds. (2007). Evidence Based Eye Care. Philadelphia, PA: Lippincott Williams & Wilkins.ISBN 0-7817-6964-7.
2. Engelgau, Michael, Linda Geiss, Jinan Saaddine, Jame Boyle, Stephanie Benjamin, Edward Gregg, Edward Tierney, Nilka Rios-Burrows, Ali Mokdad, Earl Ford, Giuseppina Imperatore, K. M. Venkat Narayan. "The Evolving Diabetes Burden in the United States." Annals of Internal Medicine, 1 June 2004. Web. 22 Apr. 2014.https://nei.nih.gov/health/diabetic/retinopathy
3. "Causes and Risk Factors". Diabetic Retinopathy. United States National Library of Medicine. 15 September 2009.
4. Expert Committee on the Diagnosis and Classification of Diabetes Mellitus (January 2003). "Report of the expert committee on the diagnosis and classification of diabetes mellitus".
5. Nonproliferative Diabetic Retinopathy (Includes Macular Edema)". Retrieved August 17, 2013.
6. R&D ACTIVITIES IN RETINAL IMAGE ANALYSIS AT CRIM Langis Gagnon, France Laliberté, Marc Lalonde R&D Department, Centre de Recherche Informatique de Montréal (CRIM) 550 Sherbrooke Street West, Suite 100, Montreal, H3A 1B9
7. B. Lay, "Analyse automatique des images angiofluorographiques au cours de la retinopathie diabetique," Ph.D. dissertation, Centre of Mathematical Morphology, Paris School of Mines, Paris, France,1983.
8. Ng, Acharya, Campilho & Suri 2014, pg. 63
9. Prevalence, risk factors and complications associated with type 2 diabetes in migrant South Asians Sara D. Garduño-Diaz and Santosh Khokhar* Version of Record online: 3 JAN 2012 DOI: 10.1002/dmrr.1219
10. Segmentation of candidate dark lesions in fundus images based on local thresholding and pixel density Enrico Grisan, Alfredo Ruggeri
11. A. D. Fleming, S. Philip, and K. A. Goatman, "Automated microaneurysm detection using local contrast normalization and local vessel detection," IEEE Trans. Med. Imag., vol. 25, no. 9, pp. 1223–1232, Sep. 2006
12. F. Zana and J. C. Klein, "Segmentation of vessel-like patterns using mathematical morphology and curvature evaluation," IEEE Trans. Image Process., vol. 10, no. 7, pp. 1010–1019, Jul. 2001.
13. T.Spencer,J.A.Olson,K.C.McHardy,P.F.Sharp,andJ.V.Forrester, "An image-processing strategy for the segmentation and quantification of microaneurysms in fluorescein angiograms of the ocular fundus," Comput.Biomed.Res., vol. 29, pp. 284–302, May 1996
14. M. J. Cree, J. A. Olson, K. C. McHardy, P. F. Sharp, and J. V. Forrester, "A fully automated comparative microaneurysm digital detection system," Eye, vol. 11, pp. 622–628, 1997.
15. A.J.Frame,P.E.Undrill,M.J.Cree,J.A.Olson,K.C.McHardy,P.F.Sharp,andJ.Forrester,"A comparison of computer based classification methods applied to the detection of microaneurysms in ophthalmic fluorescein angiograms,"Comput.Biol.Med.,vol.28,pp.225–238,1998
16. A. Mendonca, A. Campilho, and J. Nunes, "Automatic segmentation of microaneurysms in retinal angiograms of diabetic patients,"inProc. Int. Conf.ImageAnal.Process., 1999, pp. 728–733
17. A. D. Fleming, S. Philip, and K. A. Goatman, "Automated microaneurysm detection using local contrast normalization and local vessel detection," IEEE Trans. Med. Imag., vol. 25, no. 9, pp. 1223–1232, Sep. 2006.
18. M. Niemeijer, J. Staal, M. D. Abramoff, M. A. Suttorp-Schulten, and B. van Ginneken, "Automatic detection of red lesions in digital color fundus photographs," IEEE Trans. Med. Imag., vol. 24, no. 5, pp. 584–592, May 2005.
19. T. Walter, P. Massin, A. Arginay, R. Ordonez, C. Jeulin, and J. C. Klein, "Automatic detection of microaneurysms in color fundus images," Med. Image Anal., vol. 11, pp. 555–566, 2007.

20. L. Vincent, "Morphological area openings and closings for greyscale images,"inProc.NATOShapePictureWorkshop,1992,pp.197–208.
21. K. Ram, G. D. Joshi, and J. Sivaswamy, "A successive clutter-rejection-based approach for early detection of diabetic retinopathy ,"IEEE Trans.Biomed.Eng.,vol.58,no.3,pp.664–673,Mar.2011.
22. B. Zhang, X. Wu, J. You, Q. Li, and F. Karray, "Detection of microaneurysms using multi-scale correlation coefficients," Pattern Recognit., vol. 43, no. 6, pp. 2237–2248, 2010.
23. A.Mizutani,C.Muramatsu,Y.Hatanaka,S.Suemori,T.Hara,andH. Fujita, "Automated microaneurysm detection method based on double ring filter in retinal fundus images," in Proc. SPIE Med. Imag. 2009: Comput.-Aided Diagnosis, 2009, vol. 72601N.
24. G. Quellec, M. Lamard, P. Josselin, G. Cazuguel, B. Cochener, and C. Roux, "Optimal wavelet transform for the detection of microaneurysms in retinal photographs," IEEE Trans. Med. Imag., vol 27, no. 9, pp. 1230-1241, Sep. 2008.
25. C. I. Sanchez, R. Hornero, A. Mayo, and M. Garcia, "Mixture model based clustering and logistic regression for automatic detection of microaneurysms in retinal images," in Proc. SPIE Med. Imag. 2009: Comput.- Aided Diagnosis, 2009, vol. 72601M.
26. I. Lazar and A. Hajdu, "Microaneurysm detection in retinal images using a rotating cross-section based model," in IEEE Int. Symp. Biomed.Imag.:From NanotoMacro,2011,pp.1405– 1409.
27. J. Staal, M. D. Abramoff, M. Niemeijer, M. A. Viergever, and B. Van Ginneken, "Ridge based vessel segmentation in color images of the retina," IEEE Trans. Med. Imag., vol. 23, no. 4, pp. 501–509, Apr. 2004.
28. T. Zhu, "Fourier cross-sectional profile for vessel detection on retinal images,"Comput.Med.Imag.Grap.,vol.34,pp.203–212,2010.
29. E.Ricci and R.Perfetti,"Retinal blood vessel segmentation using line operators and support vector classification," IEEE Trans. Med. Imag., vol. 26, no. 10, pp. 1357–1365, Oct. 2007.
30. L. Giancardo, F. Meriaudeau, T. P. Karnowski, Y. Li, K. W. Tobin, andE.Chaum,"Microaneurysm detection with radon transform-based classification on retina images,"in Proc.IEEE Annu.Int.Conf.EMBC, 2011, pp. 5939–5942.
31. J.Lowell,A.Hunter,D.Steel,A.Basu,R.Ryder,andR.L.Kennedy, "Measurement of retinal vessel widths from fundus images based on 2-D modeling," IEEE Trans. Med. Imag., vol. 23, no. 10, pp. 1196–1204, Oct. 2004
32. I. Lazar and A. Hajdu, "Retinal Mircoaneurysm Detection Through Local Rotating Cross-Section Profile Analysis," in IEEE Int. Trans. Med.Imag, vol.32, no.2, pp.400–407, Feb 2013.
33. DIARETDB1 is Copyright © 2007 by Tomi Kauppi, Valentina Kalesnykiene, Joni-Kristian Kamarainen, Lasse Lensu, Iiris Sorri, Asta Raninen, Raija Voutilainen, Juhani Pietilä, Heikki Kälviäinen, andHannu Uusitalo <http://www.it.lut.fi/project/imageret/diaretdb1/index.html>